Self-Assembled Catalytic DNA Nanostructures for Synthesis of Para-directed Polyaniline

Zhen-Gang Wang,* Pengfei Zhan, and Baoquan Ding*

National Center for Nanoscience and Technology, Beijing 100190, P. R. China

ABSTRACT Templated synthesis has been considered as an efficient approach to produce polyaniline (PANI) nanostructures. The features of DNA molecules enable a DNA template to be an intriguing template for fabrication of emeraldine PANI. In this work, we assembled HRP-mimicking DNAzyme with different artificial DNA nanostructures, aiming to manipulate the molecular structures and morphologies of PANI nanostructures through the controlled DNA self-assembly. UV–vis absorption spectra were used to investigate the molecular structures of PANI and monitor kinetic growth of PANI. It was found that PANI was well-doped at neutral pH and the redox behaviors of the resultant PANI were dependent on the charge density of the template, which was controlled by the template configurations. CD spectra indicated that the PANI threaded tightly around the helical DNA backbone, resulting in the right handedness of PANI. These reveal the formation of the emeraldine form of PANI that was doped by the DNA. The morphologies of the resultant PANI were studied by AFM and SEM. It was concluded from the imaging and spectroscopic kinetic results that PANI grew preferably from the DNAzyme sites and then expanded over the template to form 1D PANI nanostructures. The strategy of the DNAzyme-DNA template assembly brings several advantages in the synthesis of para-coupling PANI, including the region-selective growth of PANI, facilitating the formation of a para-coupling structure and facile regulation. We believe this study contributes significantly to the fabrication of doped PANI nanopatterns with controlled complexity, and the development of DNA nanotechnology.

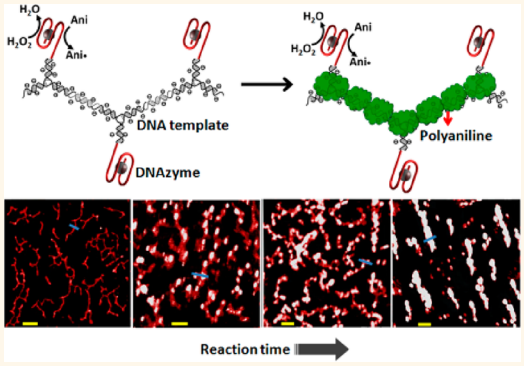

KEYWORDS: DNA · self-assembly · DNAzyme · polyaniline · emeraldine form · nanostructure

Polyaniline (PANI) has been considered as an intriguing conducting polymer, because of its facile synthesis, environmental stability, and simple acid/base doping/dedoping chemistry that could realize about a 10^{10}-fold conductivity change.[1] The electrically conducting PANI is commonly synthesized by oxidizing the aniline monomer either chemically or electrochemically[2,3] in a strong acid environment. However, the harsh synthetic conditions limited the commercial application of the resulting PANI, due to the poor solubility and processability. To solve this problem, many attempts have been made, such as self-doping methods,[4,5] mild catalyst approach,[6] and the use of polyelectrolyte as the template.[7,8]

Horseradish peroxidase (HRP) has been employed as an efficient catalyst for the polymerization of anilines.[9–11] The enzymatic approach is simple and environmentally benign; it can offer a higher degree of control over the kinetics of the reaction, and potentially fabricate a product in high yield.[9] The major drawback accompanying the HRP-catalyzed reaction is that highly branched ortho- and para-substituted PANI is generally obtained, which severely limits the degree of conjugation and hence the electrical and optical property of the resulting polymers. To minimize the parasitic branching, the HRP approach was integrated with the negatively charged polyelectrolyte to assist the polymerization of aniline.[9,10] The polyelectrolyte acts as a template on which the aniline monomers preferentially align and promote a para-directed reaction, leading to extended conjugation of the resulting PANI chains with limited parasitic branching. The template also provides the requisite counterions for charge compensation in the doping PANI

* Address correspondence to dingbq@nanoctr.cn, wangzg@nanoctr.cn.

Received for review November 22, 2012 and accepted December 28, 2012.

Published online December 28, 2012
10.1021/nn305424e

and maintains the water solubility for processing. The sulfonated polystyrene,[9] poly(acrylic acid),[12] poly(vinylphosphonic acid),[10] and DNA[11,13] have been used for the templated synthesis of PANI nanocomposites. Different from the hard template, the anionic polyelectrolyte requires no depletion from the PANI, because it can assist the PANI doping.

Among a series of the templates, DNA molecules are particularly attractive. The strict rules of base pairing, the rigidity on the nanoscale, and a near-infinite number of potential sequences have enabled DNA molecules to self-assemble into arbitrary rigid nanostructures, in the range of one dimension to three dimensions.[14−16] The progress in structural DNA nanotechnology provides the versatile negatively charged templates for the fabrication of PANI nanostructures that could copy the template morphologies. Moreover, the spatial addressability of the DNA origami template[17] offers the possibility to synthesize more complex nanopatterns confined on the scaffold. Naturally existing DNA nanostructures, calf thymus DNA, were used to template the fabrication of PANI nanowires in the homogeneous solution[13] or on the Si surface,[11] with HRP as the catalyst. HRP can work in the mild reaction environment that is required by the biological template. However, thousands of base pairs of the double-stranded calf thymus DNA is difficult to engineer. Meanwhile, the self-assembled DNA nanostructures were rarely used. Here it should be noted that in the enzymatic synthesis of PANI on the template, the procedures have to be implemented carefully, such as the dropwise addition of the oxidant (H_2O_2) with continuous stirring,[11,13,18] so that the generated aniline radical species could diffuse to the polyelectrolyte surface in time to avoid the aniline branching in the solution. This process generates difficulty for the spectroscopic monitoring of templated PANI synthesis. The kinetic study could provide the detailed information of PANI growth around the template. On the other hand, the absence of interaction between the DNA assemblies and HRP may make the template surface inefficient for formation of para-coupling PANI.

According to the Manning theory describing the counterion condensation phenomenon,[19,20] the surface pH of the negatively charged polyelectrolyte is lower than the environment. This was also demonstrated by Lochhead *et al*.[21] The low-pH surface played a significant role in directing the synthesis of the head-to-tail PANI. Accordingly, if the catalyst was anchored to the charged surface, the enzyme-generated aniline radical species could then diffuse to the charged surface quickly, facilitating the formation of head-to-tail PANI. An attempt was made by Gao *et al*. to hybridize the nucleic acid modified HRP to the overhang of a DNA duplex, to produce the assembly of HRP with the DNA duplex.[22] This method provided high charge density of the electrode surface for para-directed PANI. However, this approach is not available for producing PANI nanostructures with controlled morphologies, since the enzyme modification process usually results in a multiple DNA strands-conjugated enzyme, and the PANI nanostructures would be cross-linked. An alternative biocatalyst to HRP is the HRP-mimicking DNAzyme. It is a complex composed of iron(III)-protoporphyrin (hemin) and a DNA strand rich of guanosine bases, exhibiting the catalytic properties analogous to HRP.[23] Compared with HRP, the artificial biocatalyst can offer several advantages: (i) it can be simply engineered to include a nucleic acid sticky end for self-assembly with the DNA template. (ii) The artificial enzyme is much milder, allowing the polymerization of aniline on the charged surface upon the generation of the radical species and minimizing the parasitic branching. (iii) The activity of the mimicking enzyme can be controlled by environmental factors,[23] such as pH, metal ions (K^+ *etc*.) concentration, so that the resultant complex could still retain biocatalytic activity for further use.

In this work, we report a strategy to use DNA double-stranded (ds) template, self-assembled with DNAzyme, for the synthesis of para-directed PANI. The template for PANI synthesis ranged from a Y-shaped motif to a hundreds-of-nanometer linear nanostructure (nanowire) with controlled charged area. The effects of the template configurations on the doping behaviors of the PANI were studied. The results demonstrated that the PANI on the linear template was well-doped in neutral solution and showed desired doping/dedoping properties. The time-dependent growth of the PANI on the linear template was investigated, indicating the site-selective synthesis of PANI on the template. Although covered with PANI chains, the DNA in the complex still retains partial biological activity and is cleavable by DNAase. Moreover, the strategy to use an artificial biocatalyst assembled on the template showed a prominent feature of much more efficient synthesis of a conductive form of PANI than free-state HRP and DNAzyme. It also allows the study of the template effect on the resulting PANI.

RESULTS AND DISCUSSION

A nucleic acid strand including the G-rich sequence of HRP-mimicking DNAzyme was assembled with two complementary strands, to generate a Y-shaped DNA motif (**1**) (schematically shown in Figure 1a). In the presence of hemin, the HRP-mimicking DNAzyme was formed on the Y-shaped scaffold, which provided a counterion interface for the PANI synthesis. The polymerization process of aniline on DNAzyme-associated Y-shaped nanostructure was monitored by UV−vis spectroscopy, in Supporting Information, Figure S1a. The PANI characteristic polaron absorption bands at *ca*. 420 and 705 nm, appeared in the initial stage. As the reaction proceeded, the bands in the range of 705−400 nm were intensified. Moreover, a blue shift was observed for the absorption from 705 to 665 nm. (For the details about the growth kinetics of polyaniline, see the Supporting Information.) It was reported that

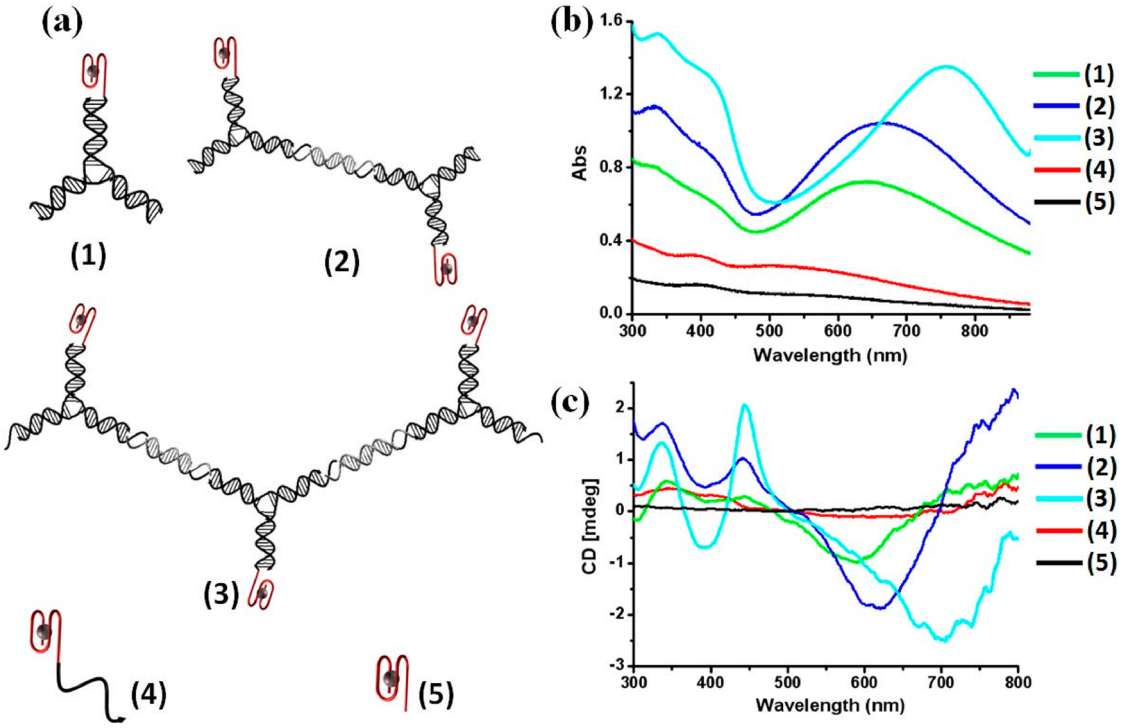

Figure 1. Synthesis of polyaniline on DNAzyme-contained DNA templates: (a) configurations of the DNA templates which templated the synthesis of PANI with different molecular structures; (b) UV−vis absorption spectra of PANI on different templates at neutral pH; (c) CD spectra of corresponding PANI.

the negatively charged polyelectrolyte can offer charge compensation in the doped PANI.[24−26] Therefore, the acidic environment of the PANI/DNA complex was neutralized to investigate the doping of PANI. The absorbance peaks at *ca.* 320, 420, and 630 nm were observed (Figure 1b), indicating existence of the conductive para-coupling emeraldine salt of PANI. Meanwhile, the reaction solution showed a blue−green color. Comparison between the solutions of pH 4.5 (fully doped, Supporting Information, Figure S1) and pH 9.8 (fully dedoped) indicates that the PANI stayed in the semidoped state in the neutral solution. DNA, existing as a right-handed helix, also acts as the chiral template for the growth of optically active PANI, which in turn provides the information of the interaction between DNA and PANI. Circular dichroism spectra (CD) were used to reveal the induced circular dichroism (ICD) of the polyanilne, shown in Figure 1c. Negative ICD peaks at 600 nm and positive peaks at 440 and 340 nm were observed, ascribing to the $\pi-\pi^*$ transition of the polaron bands and benzenoid ring in chiral PANI. These characteristic CD signals were similar to the reported results,[2] showing dependence on the template configurations (discussed later). The CD spectra demonstrate the threading of the PANI along the helical DNA template and thus adopting a preferred handedness.

Doping PANI in the neutral environment may enhance the applications in several research fields, such as biosensing and bioseparation. PANI growing on the Y-shaped DNA motif revealed semidoping behavior in the neutral environment, probably due to the loose interaction of PANI chains with a DNA backbone, resulting in the entanglement of the PANI chains. Enlarging the interaction interface between PANI and DNA may enhance the effect of dopant charges on PANI doping. Therefore, two units of the Y-shaped motif were bridged by a spacer, to create a template (**2**) with more negatively charged interface for PANI growth, schematically shown in Figure 1a. The PANI absorbance at neutral solution showed a stronger characteristic absorbance at *ca.* 320 and 420 nm, as well as the red shift of the band in the range of 600−700 nm, compared to the Y-shaped motif (**1**) (Figure 1b). It reveals the PANI was more doped for the bridged Y-shape motifs than that on single Y-shaped DNA motif, at neutral pH. Stronger CD peaks at corresponding wavelength were also observed, ascribed to the stronger interaction between PANI and DNA backbone (Figure 1c, blue line). On the basis of this concept, the counterions interface was further enlarged by bridging both nonbiocatalytic ends of the Y-shaped units to form a DNA linear structure (**3**), schematically shown in Figure 1a. The structure (**3**) was produced through stepwise assembly of (**1**) and the spacer motif (see the Supporting Information). The time-dependent UV−vis spectra show a different behavior of PANI growth from the motif (**1**). The absorbance in the range of 600−800 nm underwent blue- and red-shift process (705 → 660 → 710 nm) (see Supporting Information, Figure S1b). It should be noted that the spectroscopic

investigation was only conducted in the initial *ca*. 14 h of the growth, and after *ca*. 40h, the green precipitates appeared. The structure (**3**)-templated PANI showed stronger characteristic absorption of the doped PANI than (**1**) and (**2**), as shown in Figure 1b, revealing the significant role of DNA in templating the formation of emeraldine form. The CD spectrum shows the strong peaks corresponding to UV−vis absorption, and it is ascribed to the tight threading of PANI around the DNA chain. To further demonstrate the DNA-dependent doping behaviors of the PANI, a DNAzyme bearing a single strand (40 nt), (**4**) and a pure DNAzyme sequence, (**5**) were used as the template for the PANI synthesis. The configurations of (**4**) and (**5**) are shown in Figure 1a. No characteristic absorption of the emeraldine form of the PANI appeared, and the precipitation of brown product was observed. The branched structure of the PANI probably resulted from the insufficient charged surface.

The results above imply a relationship between the charged surface and the doping behaviors of the resulting PANI. This inspires us to further investigate the role of interfacial charge density in the doped behavior of PANI. Therefore, a series of DNA nanostructures were assembled around the catalytic DNAzyme sites. These structures are designed to include similar configurations so that the charge density around the DNAzyme increases as the number of DNA bases. The configuration of the templates and the resulting absorption spectra are shown in Supporting Information, Figure S2. At neutral pH, as the number of duplex units increased and the characteristics of the emeraldine forms became stronger. The absorption spectrum of PANI growing on (**10**) is comparable with (**3**). This indicates that the molecular structure as well as the doping behavior of the synthesized PANI was dependent on the charge density. It demonstrates an approach of controlling the synthesis of PANI through facile manipulation of the template assembly.

To investigate the advantage of the assembly of DNAzyme, an experiment was implemented to compare PANI synthesized in solution I (including DNA template (**3**)/assembled DNAzyme**)** with solution II (including DNA template and freely diffusing DNAzyme or solution III (including DNA template and free-diffusing HRP), schematically shown in Supporting Information, Figure S3. During the reaction, it was found that the solution I turned green gradually, while the solution II turned brown with the simultaneous addition of aniline and H_2O_2. For the solution III, H_2O_2 was added dropwisely as reported,[9,13] and the solution turned dark purple. The comparison demonstrates that the strategy of assembling DNAzyme with the template is highly advantageous in the synthesis of para-coupling PANI, due to the efficient interaction between the enzyme and the polymerization scaffold. For the sequences assembling the nanostructures, see the Supporting Information.

The reversible redox behavior of the PANI was studied by dedoping and redoping using $NH_3 \cdot H_2O$ and acetic acid (HAc). According to the growth kinetics of the PANI, it is concluded that the PANI synthesized on (**3**) could show different doping properties from that on (**1**). Therefore, it will be of interest to investigate the dedoping/doping process of the PANI on different templates. The spectra of stepwise dedoping and doping of (**3**)-templated PANI are shown in Figure 2a (left). As pH increased, a decrease and subsequent disappearance of the polaron bands at 420 nm, and the enhanced $\pi-\pi^*$ transition of the benzenoid rings at 320 nm were observed, similar to that on (**1**) and (**2**) (for the dedoping and redoping of PANI/(**1**) and PANI/(**2**), see Supporting Information, Figure S4). However, the shift of the bands in the range of 500−800 nm experienced different processes. For (**1**)/PANI complex, a gradual blue shift was observed for maximum absorption wavelength of 640−570 nm. The dedoping of (**3**)/PANI complex showed a gradual decrease and increase of the absorbance at 770 nm (polaron bands) and 570 nm (due to excitation transition of the quinoid rings), respectively, the typical features of para-directed PANI dedoping.[9] In the middle of the dedoping process (see the inset), two characteristic absorption bands appeared, suggesting the coexistence of the quinoid and benzenoid rings (semiquinoid). Furthermore, isosbestic points at 338, 465, and 632 nm can be observed clearly, which was also shown previously in a sulfonic acid ring-substituted PANI system.[27,28] The dedoping of PANI templated by (**2**) revealed the kinetic transformation of absorption wavelength with the characteristics between (**1**) and (**3**). The base form of PANI can be redoped to the emeraldine salt through titration with HAc, and the spectra are shown in Figure 2a (right). A reversible color change, between green and purple, was observed. The pH induced redox reversibility confirms the presence of the electroactive form of PANI in the PANI/DNA complex. Interestingly, after the (**3**)/PANI complex was treated by fast annealing, the spectrum (Supporting Information, Figure S5) shows the characteristic absorption of semiquinoid analogous to the middle stage of the dedoping process (inset of Figure 2a), observed as a blue−green color. The molecular weight of PANI cannot be changed by the thermal treatment. Instead, the molecular weight of the template (**3**) was decreased by the annealing, demonstrated by agarose gel electrophoresis (not shown). Therefore, it is concluded that the dopant role of the DNA was weakened because of the thermal treatment, changing the doping state of the PANI.

The pH-dependent CD spectra of (**3**)/PANI are used to investigate the chirality of PANI during doping and dedoping (Figure 2b). As pH increased, a blue shift of the CD peak in the range of 700−800 nm was observed; the peaks at 440 nm disappeared gradually, which was consistent with the UV spectrum. After redoping, the CD spectrum was recovered. The helical conformation of PANI was retained when the PANI was

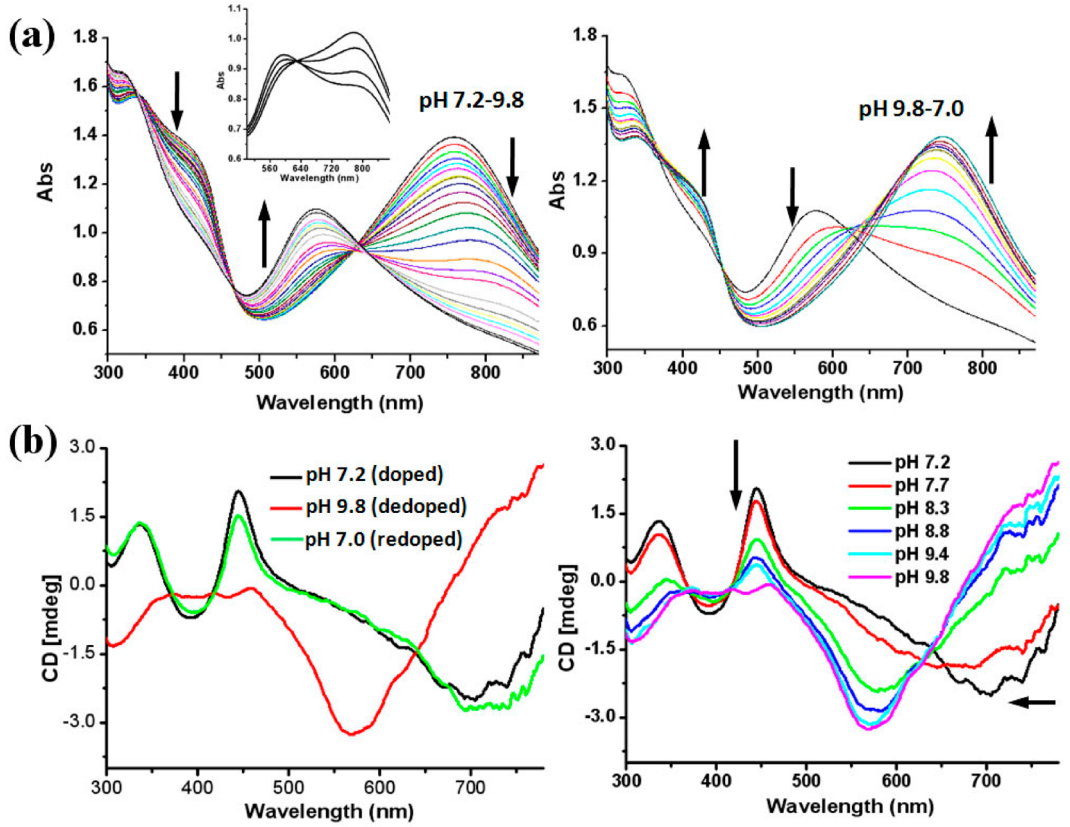

Figure 2. Dedoping and redoping of PANI synthesized on template (5): (a) UV−vis spectra of dedoping (left, the inset represents the middle stage of the dedoping process) and redoping (right); (b) CD spectra of doped, dedoped, and redoped PANI (left) and dedoping process (right).

dedoped and redoped, during which the interaction between PANI and the DNA backbone stayed intact. This experiment demonstrates the resulting molecular structures, and the doping/dedoping behaviors of PANI were dependent on the charge density, in other words, the nanostructure of the DNA template.

The assembly of (**1**) with bridging DNA units generated a 1D duplex nanostructure which was subsequently used for the synthesis of PANI nanowire. In the process of enzymatic polymerization of aniline, the aniline radicals are oxidized from aniline by intermediate species of the enzyme. These free radicals undergo coupling to produce the dimer, and successive oxidization and coupling reactions eventually result in the formation of polymer wires. The "Manning theory" allows the para coupling of aniline on the negatively charged surface of the polyelectrolyte, DNA, under reaction conditions. We speculate that the PANI starts to grow around the DNAzyme preferentially, since the aniline radicals generated by the DNAzyme could diffuse to the areas more adjacent to the DNAzyme site. Figure 3 shows the AFM images of the growth of PANI on the DNA nanostructure at different time stages. The apparent height of the linear DNA template was *ca.* 2.2 nm, consistent with the formation of duplex DNA. After 20 min of reaction, the height of the partial area increased to 5−7 nm (shown as white region), indicating the formation of PANI threading around the DNA backbone, while the height of the other regions of the nanostructure remained as the height of the duplex. In the crop figure, PANI aggregates were in an equidistant arrangement. The distance between the PANI aggregates was *ca.* 37 nm, approximately the distance between the centers of Y subunits (122 base pairs and *ca.* 36.6 nm). This indicates DNAzyme guided the growth of PANI around the enzyme location. After 90 min, the height of the nanowires remained as the same height, while the length expanded, indicating the continuous growth of PANI on the DNA nanostructure. After 4 h reaction, nearly all of the DNA backbone was covered with PANI, with a height of 15−18 nm. The formation of the PANI wires was further conformed by SEM images (Supporting Information, Figure S6) which illustrated the successful synthesis of PANI nanostructures on the template of DNAzyme-encoded DNA nanoassemblies. The region-selective growth of PANI was also demonstrated by the spectrum that showed growth kinetics of PANI on (**3**) (see Supporting Information, Figure S1b). The initial stage was analogous to PANI synthesis on (**1**), that is, the blue shift of the absorption at 600−800 nm. Then the red shift of the absorption was observed until the precipitation of the product. The shifts imply that PANI in the beginning grew on the DNAzyme-contained Y subunit. It resulted in the gradual branching of PANI due to the decreasing DNA−PANI interactions. Subsequently, the growth of

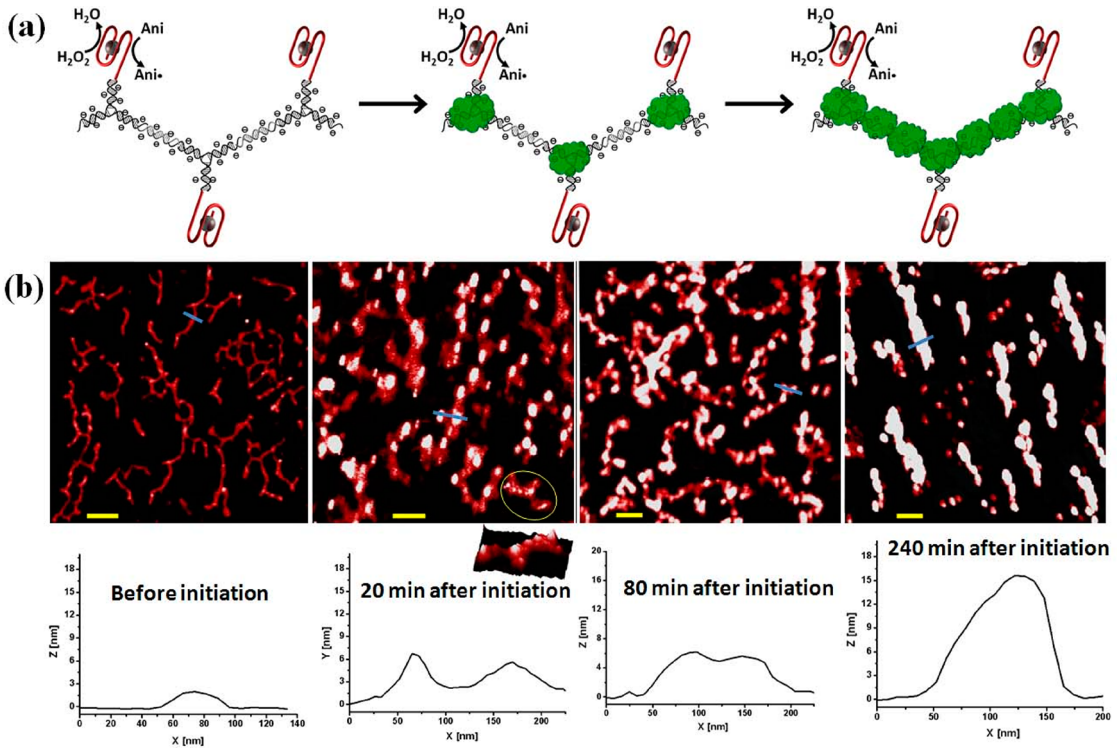

Figure 3. DNAzyme guided region-selective growth of PANI: (a) schemes of the growth process; (b) AFM monitoring of the PANI growth. Bottom panels show the height of the corresponding cross section.

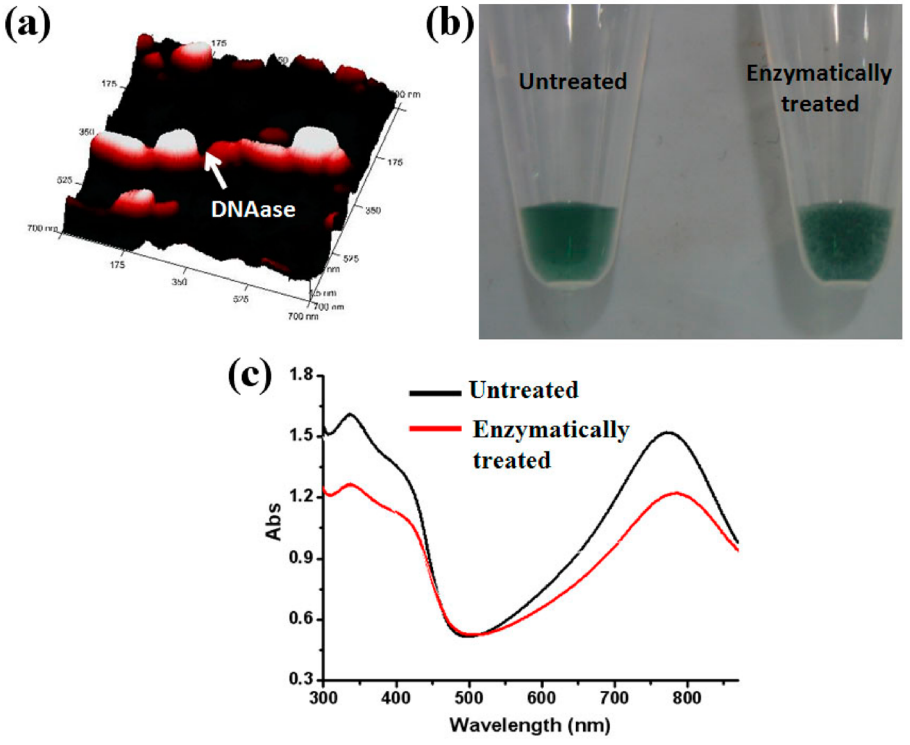

Figure 4. Enzymatic treatment of the PANI/DNA complex: (a) 3D AFM image of the digestion site of PANI/DNA complex by DNAase; (b) solutions of untreated and enzymatically treated PANI/DNA complexes; (c) UV−vis absorption spectra.

PANI expanded to other DNA chains, leading to the extended conjugation length of the PANI. The kinetic results provide the further evidence for the region-selective growth of PANI on the linear template.

The PANI wire, existing as emeraldine salt or base form, was partially soluble in aqueous solution, although it precipitates after 4 h. The 3D AFM image of the PANI/DNA complex (Figure 4a) indicates that the linear

structure of the DNA duplex was not uniformly wrapped by the PANI, showing that the exposure of the DNA chain could contribute to the water solubility of the insoluble PANI. The role of DNA in the PANI solubility was further investigated by an enzymatic digestion experiment. DNase I was added to the PANI/DNA complex solution, and the green precipitates appeared (Figure 4b). This reveals that the exposed DNA chain was digested by the enzyme, and the PANI interacted directly with the water, resulting in the insolubility of the complex. However, in such a solution condition (pH 7.0), the UV−vis absorption spectrum shows the PANI was still in the doped state, shown in Figure 4c. This is ascribed to the dopant ions of DNA embedded in the PANI. This digestion experiment demonstrates the role of DNA in the solubility of PAN nanostructures, as well as the biological activity of the DNA/PANI complex toward DNAase.

CONCLUSIONS

In summary, a novel catalytic route for the fabrication of water-soluble PANI is presented. HRP mimicking DNAzyme that assembled on DNA nanostructures was used for the catalytic reaction. This artificial enzyme shows several advantages. (i) The DNA-encoded enzyme can be engineered with a nucleic tether that is self-assembled within the template, so that the growth region of PANI can be controlled. (ii) The coassembly of the relatively milder enzyme with the template allows the generated aniline radicals to diffuse to the charged template surface quickly, thus obviating the formation of branched polymer. (iii) The emeraldine form of PANI can be synthesized on predesigned DNA nanostructures with controlled regularity and doping behaviors, and the PANI can be doped and dedoped reversibly between neutral and basic pH. These features allow studying the growth kinetics of PANI on the polyelectrolyte template. On the other hand, they offer promise for the growth of the complex PANI patterns on a 2D or 3D template surface, with rational arrangement of the enzyme sites. Moreover, the retention of DNA biological activity and the right-handed PANI offers the potential application of DNA/PANI complex nanostructures in biological fields.

METHODS

Materials. All DNA oligonucleotides were purchased from Invitrogen Life Technologies (Shanghai, China) and purified by polyacrylamide gel electrophoresis. Aniline (99%) and hemin chloride (98) were purchased from Alfa Aesar. All other chemicals and solvents used were also commercially available, of analytical grade or better, and used as received.

Assembly of DNA templates: Y-shaped DNA motif (**1**) and the bridging motif (*the duplex with sticky ends to bridge the Y-shaped motifs*) were assembled by annealing the composing DNA strands from 90 °C to room temperature in the phosphate buffer (phosphate buffer saline 30 mM, [Na^+] 54 mM, pH 7.2. This buffer was used through this work). The assembly of linear nanostructure (**3**) was performed in a stepwise approach. In the beginning one unit of Y motif and two units of bridging motif were mixed in the phosphate buffer at room temperature for 1 h. Then, two units of Y motif and bridging motif were added successively, to produce the linear template. The resulting solution included 24 units of the bridging motifs and 23 units of the Y-shaped motifs.

Synthesis of PANI. The solution, including template (**1**), (**2**), or (**3**), was acidified to pH 4.5 by the addition of aniline solution (aniline was predissolved in acetic acid aqueous solution) and H_2O_2. The resulting solution included a Y-shaped motif of 2.0 μM, the bridging motif of 2.0 μM, aniline of 40 mM, and H_2O_2 of 40 mM. The synthesis of PANI was initiated by the addition of hemin (10.0 μM) to the mixture. The samples for AFM imaging and SEM imaging were taken from the reaction solution at the required time stage. The precipitation indicated the termination of the reaction. Then, the precipitate was washed and transferred to the phosphate buffer. $NH_3 \cdot H_2O$ and acetic acid aqueous solution were used to dedope and redope the PANI.

Characterizations. Atomic force microscopy (AFM) imaging was performed at room temperature using a multimode scanning probe microscope with a Nanoscope 3A controller (Veeco Probes, USA). For AFM topology imaging, 5 μL of reaction solution was deposited on freshly cleaved mica surfaces, gently washed with double distilled water, and dried under a nitrogen flow. Mica surfaces were preactivated with $MgCl_2$ for 5 min and then washed with double distilled water. Images were recorded with SNL10 AFM tips (Bruker, USA) using the tapping mode at their resonant frequency. The images were analyzed using Nanoscope Analysis software.

The morphology of the resulting PANI, which was deposited on an Si wafer, was also examined by SEM (Hitachi S-4800). The CD (JACO J810) and UV−vis (Shimadzu) spectra were recorded for PANI dispersed in phosphate buffer (pH 7.2).

Conflict of Interest: The authors declare no competing financial interest.

Acknowledgment. The authors are grateful for the financial support from National Science Foundation China (51203031, 21173059, 21222311, 91127021 and 21205022), National Basic Research Program of China (973 Program, 2012CB934000), 100-Talent Program of Chinese Academy of Sciences (B.Q.D), Beijing Natural Science Foundation (2122057).

Supporting Information Available: Sequences used for the DNA templates, schematic assembly process of template (**3**) and Figure S1−S6. This material is available free of charge *via* the Internet at http://pubs.acs.org.

REFERENCES AND NOTES

1. Li, D.; Huang, J. X.; Kaner, R. B. Polyaniline Nanofibers: A Unique Polymer Nanostructure for Versatile Applications. *Acc. Chem. Res.* **2009**, *42*, 135–145.
2. Kane-Maguire, L. A. P.; Wallace, G. G. Chiral Conducting Polymers. *Chem. Soc. Rev.* **2010**, *39*, 2545–2576.
3. Wei, Z. X.; Faul, C. F. J. Aniline Oligomers-Architecture, Function and New Opportunities for Nanostructured Materials. *Macromol. Rapid Commun.* **2008**, *29*, 280–292.
4. Lin, H. K.; Chen, S. A. Synthesis of New Water-Soluble Self-Doped Polyaniline. *Macromolecules* **2000**, *33*, 8117–8118.
5. Bae, W. J.; Kim, K. H.; Park, Y. H.; Jo, W. H. A Novel Water-Soluble and Self-Doped Conducting Polyaniline Graft Copolymer. *Chem. Commun.* **2003**, 2768–2769.
6. Xu, P.; Singh, A.; Kaplan, D. L. Enzymatic Catalysis in the Synthesis of Polyanilines and Derivatives of Polyanilines. *Adv. Polym. Sci.* **2006**, *194*, 69–94.
7. Li, W. G.; McCarthy, P. A.; Liu, D. G.; Huang, J. Y.; Yang, S. C.; Wang, H. L. Toward Understanding and Optimizing the

Template-Guided Synthesis of Chiral Polyaniline Nanocomposites. *Macromolecules* **2002**, *35*, 9975–9982.
8. Wang, W.; Lu, X. F.; Li, Z. Y.; Lei, J. Y.; Liu, X. C.; Wang, Z. J.; Zhang, H. N.; Wang, C. One-Dimensional Polyelectrolyte/Polymeric Semiconductor Core/Shell Structure: Sulfonated Poly(arylene ether ketone)/Polyaniline Nanofibers for Organic Field-Effect Transistors. *Adv. Mater.* **2011**, *23*, 5109–5112.
9. Liu, W.; Kumar, J.; Tripathy, S.; Senecal, K. J.; Samuelson, L. Enzymatically Synthesized Conducting Polyaniline. *J. Am. Chem. Soc.* **1999**, *121*, 71–78.
10. Nagarajan, R.; Tripathy, S.; Kumar, J.; Bruno, F. F.; Samuelson, L. An Enzymatically Synthesized Conducting Molecular Complex of Polyaniline and Poly(vinylphosphonic acid). *Macromolecules* **2000**, *33*, 9542–9547.
11. Ma, Y. F.; Zhang, J. M.; Zhang, G. J.; He, H. X. Polyaniline Nanowires on Si Surfaces Fabricated with DNA Templates. *J. Am. Chem. Soc.* **2004**, *126*, 7097–7101.
12. Thiyagarajan, M.; Samuelson, L. A.; Kumar, J.; Cholli, A. L. Helical Conformational Specificity of Enzymatically Synthesized Water-Soluble Conducting Polyaniline Nanocomposites. *J. Am. Chem. Soc.* **2003**, *125*, 11502–11503.
13. Nagarajan, R.; Liu, W.; Kumar, J.; Tripathy, S. K.; Bruno, F. F.; Samuelson, L. A. Manipulating DNA Conformation Using Intertwined Conducting Polymer Chains. *Macromolecules* **2001**, *34*, 3921–3927.
14. Aldaye, F. A.; Palmer, A. L.; Sleiman, H. F. Assembling Materials with DNA as the Guide. *Science* **2008**, *321*, 1795–1799.
15. Wilner, O. I.; Willner, I. Functionalized DNA Nanostructures. *Chem. Rev.* **2012**, *112*, 2528–2556.
16. Seeman, N. C. Structural DNA Nanotechnology: Growing along with Nano Letters. *Nano Lett.* **2010**, *10*, 1971–1978.
17. Nangreave, J.; Han, D. R.; Liu, Y.; Yan, H. DNA Origami: A History and Current Perspective. *Curr. Opin. Chem. Biol.* **2010**, *14*, 608–615.
18. Nickels, P.; Dittmer, W. U.; Beyer, S.; Kotthaus, J. P.; Simmel, F. C. Polyaniline Nanowire Synthesis Templated by DNA. *Nanotechnology* **2004**, *15*, 1524–1529.
19. Manning, G. S. Limiting Laws and Counterion Condensation in Polyelectrolyte Solutions .I. Colligative Properties. *J. Chem. Phys.* **1969**, *51*, 924–&.
20. Manning, G. S. Counterion Binding in Polyelectrolyte Theory. *Acc. Chem. Res.* **1979**, *12*, 443–449.
21. Lochhead, M. J.; Letellier, S. R.; Vogel, V. Assessing the Role of Interfacial Electrostatics in Oriented Mineral Nucleation at Charged Organic Monolayers. *J. Phys. Chem. B* **1997**, *101*, 10821–10827.
22. Gao, Z. Q.; Rafea, S.; Lim, L. H. Detection of Nucleic Acids Using Enzyme-Catalyzed Template-Guided Deposition of Polyaniline. *Adv. Mater.* **2007**, *19*, 602–606.
23. Travascio, P.; Li, Y. F.; Sen, D. DNA-Enhanced Peroxidase Activity of a DNA Aptamer-Hemin Complex. *Chem. Biol.* **1998**, *5*, 505–517.
24. Tian, S. J.; Liu, J. Y.; Zhu, T.; Knoll, W. Polyaniline Doped with Modified Gold Nanoparticles and Its Electrochemical Properties in Neutral Aqueous Solution. *Chem. Commun.* **2003**, 2738–2739.
25. Bartlett, P. N.; Simon, E. Poly(aniline)-poly(acrylate) Composite Films as Modified Electrodes for the Oxidation of NADH. *Phys. Chem. Chem. Phys.* **2000**, *2*, 2599–2606.
26. Xiao, Y.; Kharitonov, A. B.; Patolsky, F.; Weizmann, Y.; Willner, I. Electrocatalytic Intercalator-Induced Winding of Double-Stranded DNA with Polyaniline. *Chem. Commun.* **2003**, 1540–1541.
27. Chen, S. A.; Hwang, G. W. Structure Characterization of Self-Acid-Doped Sulfonic Acid Ring-Substituted Polyaniline in Its Aqueous Solutions and as Solid Film. *Macromolecules* **1996**, *29*, 3950–3955.
28. Chen, S. A.; Hwang, G. W. Water-Soluble Self-Acid-Doped Conducting Polyaniline- Structure and Properties. *J. Am. Chem. Soc.* **1995**, *117*, 10055–10062.